RESEARCH PAPER

Effect of Microstructure on Stress Dependence of Transformation Induced Plasticity in TRIP800 Low-Alloy Multiphase Steels

F. Hosseinabadi[1], A. Rezaee-Bazzaz[1*], M. Mazinani[1] and B. Mohammad Sadeghi[2]

** bazaz-r@um.ac.ir*

Received: February 2019 **Revised: September 2019** **Accepted: November 2019**

[1] Department of Metallurgy and Materials Engineering, Faculty of Engineering, Ferdowsi University of Mashhad, Mashhad, Iran.

[2] School of Metallurgy and Materials Engineering, Iran University of Science and Technology, Tehran, Iran.

DOI: 10.22068/ijmse.17.1.109

Abstract: *An experimental–numerical methodology was used in order to study the microstructural effects on stress state dependency of martensitic transformation kinetics in two different TRIP800 low alloy multiphase steels. Representative volume elements extracted from actual=microstructure were utilized to stimulate the mechanical behavior of above mentioned steels. The mechanical behavior for each constituent phases required in the model was taken out from those reported in the literature. A stress invariant based transformation kinetics law was used to predict the martensitic phase transformation during deformation. Crystallographic and thermodynamic theories of martensitic phase transformation were utilized to estimate the constant parameters of the kinetics law, in a recently performed investigation. However, the sensitivity of the transformation to the stress state remained as an adjustable parameter. The results of the current work show that the stress state sensitivity of martensitic phase transformation in the investigated steels is microstructure-dependent and the value of this parameter is almost equal to half of the bainite volume fraction. Therefore, the volume fraction of bainite in the low-alloy multiphase TRIP800 steels can be used as a first postulation to determine the value of the martensitic phase transformation sensitivity to the stress state. The microstructure based model previously developed for calculating the mechanical behavior of the TRIP800 steels can be utilized as a virtual design tool for the development of TRIP steels having specific mechanical properties.*

Keywords: *Duplex Stainless Steel, Heat Treatment, Aging, Microstructure, Electrochemical Behaviors, Hardness.*

1. INTRODUCTION

Low alloy TRIP steels are known as an important class of low alloy high strength steels with a multiphase microstructure consisting of bainite and retained austenite within the ferrite matrix. These steels have desirable combination of high strength and good ductility because of strain induced martensitic transformation of metastable retained austenite [1].

The suitable combination of strength and ductility of TRIP steels makes them good candidates for potential application in automobile industries to improve crash worthiness accompanied by weight reduction. Mechanical properties of multiphase TRIP steels are thoroughly related to their microstructure. Consequently, estimation of these properties in a microscopic level seems to be rational. A number of micromechanical models have been exploited to simulate local deformation behavior of TRIP steels. Estimation of micro-stress and micro-strain distribution within and around plate shape martensitic variants [2], prediction of the onset and/or the kinetics of strain induced martensitic transformation by the use of a thermodynamic transformation criterion [3], simulation of transformation induced plasticity by determination of plastic strain induced in a spherical parent phase by the growth of a spherical transformation product phase core [4-6] and modeling of M_s temperature shift under different loading circumstances, assuming strain induced martensitic phase transformation as a nucleation–controlled phenomenon [7] are among the researches in which micromechanics based method for simulation of localized deformation in TRIP steels have been utilized.

Although the aforementioned investigations provide useful information about the mechanical behavior of TRIP steels, some important features in deformation behavior of these materials such as ultimate strength and ultimate ductility still cannot

[DOI: 10.22068/ijmse.17.1.109]

be predicted by these models. This inadequacy has been eliminated in recent investigations in which the representative volume element, based on the actual microstructure has been considered for estimating mechanical properties of multiphase TRIP steels [8-10].

A developed stress invariant-based transformation kinetics law were used to capture the martensitic phase transformation throughout deformation in the actual microstructure-based studies [11, 12]. The stress invariant transformation equation contains four different parameters which should be determined to predict the overall accumulative deformation behavior of TRIP steels. These parameters were considered as the adjusting parameters in the actual microstructure-based investigations which were reviewed in the above paragraph. The theoretical calculation of these parameters have been developed by the others, previously [13]. It has been shown that all of the constants can be theoretically calculated except the sensitivity of the transformation to the stress state which should still be considered as an adjusting parameter in of model. The results of the work done on the effect of stress state on the strain induced martensitic phase transformation show that various TRIP assisted steels with different microstructures even those with the same chemical compositions exhibit different stress state sensitivities [14-17]. Therefore, it seems that the study of microstructure dependency of stress state sensitivity of strain induced martensitic phase transformation is essential and will be attempted in the current research work. The microstructure based finite element model considering the stress invariant martensitic transformation kinetics law has been already used as a virtual design tool for investigating the influence of various design parameters on the deformation behavior of TRIP steels [18]. In the latter study, each constant of the stress invariant martensitic kinetics law was changed independently and the effects of these modifications on the mechanical properties of the TRIP steels were investigated. Although the effect of microstructure on the mechanical behavior of TRIP steels were also studied in this research, the kinetics law constants were considered as the adjusting parameters and were independent of, chemical composition, crystallographic parameters of austenite and martensite phases and the microstructure which was in disagreement with previous studies [13-17]. Therefore, the effect of changes in stress invariant martensitic kinetics law constants on the mechanical properties of TRIP steels reported in the literature needs to be reconsidered. Study of microstructure dependency of stress state sensitivity of strain induced martensitic phase transformation and reconsideration of the previously reported effects of martensitic kinetics law constants change on the mechanical behavior of TRIP steels are the main novelty of the current investigation.

2. KINETICS OF MARTENSITIC PHASE TRANSFORMATION

The modified and generalized model of transformation induced martensitic phase transformation kinetics utilized in the recently conducted studies on micromechanical simulation of TRIP800 steels, were used in the current work as well [8-10]. This model which has already been described in detail previously [13], is briefly reviewed for the sake of completeness.

The martensitic domain formation is possible whenever the associated driving force reaches the critical energy barrier for the transformation [11]. The macroscopic mechanical driving force of martensitic transformation as expressed in the following equation [11, 12], has been utilized to predict the transformation kinetics,

$$\bar{\sigma}^{A} : \tilde{\varepsilon}^{tr} = R\sqrt{3J_2}\left[1 + k\frac{J_3}{J_2^{3/2}}\right] + \frac{\alpha I_1}{3} \qquad (1)$$

Where, $\bar{\sigma}^{A}$ is the average stress in the austenite phase, $\tilde{\varepsilon}^{tr}$ denotes the average transformation strain, R corresponds to the maximum transformation shear strain, k describes the sensitivity of the transformation to the stress state, α is the volume strain accompanied by the martensitic transformation, I_1 is the first invariant of stress tensor, J_2 and J_3 are the second and third invariants of deviatoric stress tensor, respectively.

The values of parameters R and α in equation 1 can be calculated theoretically based on the crystallographic description of martensitic transformation stated previously [19- 20].

[DOI: 10.22068/ijmse.17.1.109]

During the martensitic phase transformation of ferrous alloys, FCC crystal structure of the parent phase (austenite) – changes into BCT structure of the product (martensite). The Bain strain, i.e. the strain corresponding to the transformation of a unit cell in the parent crystal structure into the product with the smallest atomic displacement, can be obtained by the following equation [19, 20]:

$$(\gamma B\gamma)=\begin{bmatrix}\eta_1 & 0 & 0\\ 0 & \eta_2 & 0\\ 0 & 0 & \eta_3\end{bmatrix} \quad (2)$$

Where, $\eta_1=\eta_2=\sqrt{2}\left(\frac{a_\delta}{a_\gamma}\right)$ and $\eta_3=\frac{c_\delta}{a_\gamma}$. The subscripts γ and α′ denote the austenite and martensite phases, respectively. *a* and *c* are the lattice parameters of corresponding crystal structure.

Since the invariant line of the martensitic transformation strain should be on the $\{110\}$ planes of the austenite phase which do not contain the *c* axis of the martensite [21], the plane defined by the invariant–normal of the transformation strain should contain one of the $<1\bar{1}1>$ directions. Assuming (101) and $[10\ \bar{1}]$ to be, the plane containing the invariant line and the direction lying on the invariant–normal plane of the transformation strain, the unit vector on the invariant line, $[u_1\,u_2\,u_3]$, can be calculated [13]. The vector $[u_1\,u_2\,u_3]$ changes into a new vector $[v_1\,v_2\,v_3]$ because of the Bain transformation. Therefore:

$$[v_1\,v_2\,v_3]=[u_1\,u_2\,u_3]\,(\gamma B\gamma) \quad (3)$$

The vector $[u_1\,u_2\,u_3]$ has already been considered to be an invariant vector and thus, its length should remained unchanged after the Bain deformation. Using equation 3 and the length invariance of the $[u_1\,u_2\,u_3]$ vector, $[v_1\,v_2\,v_3]$ can be determined [13]. Based on the assumption that the plane indicated by $(h_1\,h_2\,h_3)$ contains $[10\ \bar{1}]$ direction, the invariant unit vector perpendicular to the invariant line, i.e. $[h_1\,h_2\,h_3]$ can be calculated [13]. This direction becomes the new vector $[l_1\,l_2\,l_3]$ as a result of the Bain transformation. Therefore:

$$[l_1\,l_2\,l_3]=[h_1\,h_2\,h_3]\,(\gamma B\gamma)^{-1} \quad (4)$$

Using equation 4 and the invariance of $[h_1\,h_2\,h_3]$, the $[l_1\,l_2\,l_3]$ vector is calculated [13].

One way to convert $(\gamma B\gamma)$ into an invariant strain is to employ a rigid body rotation which rotates simultaneously $[l_1\,l_2\,l_3]$ into $[h_1\,h_2\,h_3]$ and $[v_1\,v_2\,v_3]$ into $[u_1\,u_2\,u_3]$. Defining the $[a_1\,a_2\,a_3]$ vector as the cross product of $[u_1\,u_2\,u_3]$ and $[h_1\,h_2\,h_3]$ vectors and considering the $[b_1\,b_2\,b_3]$ vector to be the cross product of $[v_1\,v_2\,v_3]$ and $[l_1\,l_2\,l_3]$ vectors, this rigid body rotation can be expressed as

$$(\gamma J\gamma)=\begin{pmatrix}u_1 & h_1 & a_1\\ u_2 & h_2 & a_2\\ u_3 & h_3 & a_3\end{pmatrix}\begin{pmatrix}v_1 & l_1 & b_1\\ v_2 & l_2 & b_2\\ v_3 & l_3 & b_3\end{pmatrix}^{-1} \quad (5)$$

Therefore, the invariant line strain can be obtained as follows

$$(\gamma S\gamma) = (\gamma J\gamma)\,(\gamma B\gamma) \quad (6)$$

The invariant line strain, $(\gamma S\gamma)$, should be factorized according to the following equation to obtain the shape deformation matrix, $(\gamma P\gamma)$.

$$(\gamma S\gamma) = (\gamma P\gamma)\,(\gamma Q\gamma) \quad (7)$$

where

$$(\gamma P\gamma)=\begin{pmatrix}1+md_1p_1 & md_1p_2 & md_1p_3\\ md_2p_1 & 1+md_2p_2 & md_2p_3\\ md_3p_1 & md_3p_2 & 1+md_3p_3\end{pmatrix} \quad (8)$$

and

$$(\gamma Q\gamma)=\begin{pmatrix}1+ne_1q_1 & ne_1q_2 & ne_1q_3\\ ne_2q_1 & 1+ne_2q_2 & ne_2q_3\\ ne_3q_1 & ne_3q_2 & 1+ne_3q_3\end{pmatrix} \quad (9)$$

In Equation 8, $[d_1\,d_2\,d_3]$ and $[p_1\,p_2\,p_3]$ are the unit vectors in the direction of macroscopic displacement and the normal of the invariant plane of the transformation, respectively. The magnitude of displacement due to the martensitic transformation is represented by m. Since he lattice invariant shear has been assumed to occur on $(101)[\bar{1}01]$ system and its effect is to cancel the shape change due to *(γQγ)* according to the phenomenological theory of martensite phase transformation, the latter should

[DOI: 10.22068/ijmse.17.1.109]

be a shear on $(101)[\bar{1}01]$. Therefore, $[q_1\, q_2\, q_3]$ equals $[0.707\ 0\ 0.707]$ and $[e_1\, e_2\, e_3]$ can be expressed as $[0.707\ 0\ -0.707]$ [19, 20]. Using Equations 5 - 8 and based on the knowledge of the $[q_1\, q_2\, q_3]$, $[e_1\, e_2\, e_3]$ and $(\gamma S\gamma)$, $[d_1\, d_2\, d_3]$ vector can be determined by mathematical calculations [13]. It is worth noting that since $(\gamma J\gamma)$ and $(\gamma B\gamma)$ are known, $(\gamma S\gamma)$ is obtainable.

From Equation 6, it is clear that

$$(\gamma S\gamma)^{-1} = (\gamma Q\gamma)^{-1}(\gamma P\gamma)^{-1} \tag{10}$$

Using Equation 10 and the value of $[d_1\, d_2\, d_3]$, $[mp_1\, mp_2\, mp_3]$ can be calculated [13]. Knowing that $[p_1\ p_2\ p_3]$ (normal of the habit plane) is a unit vector, the value of m is obtainable.

The values of α and R can be calculated using the following equations:

$$\alpha = (p_1\ p_2\ p_3).\begin{bmatrix} md_1 \\ md_2 \\ md_3 \end{bmatrix} \tag{11}$$

$$R = (m^2 - \alpha^2)^{\left(\frac{1}{2}\right)} \tag{12}$$

α, R and m parameters together with the indices d_1, d_2 and d_3 in $[d_1\, d_2\, d_3]$ vector are illustrated schematically in Fig. 1.

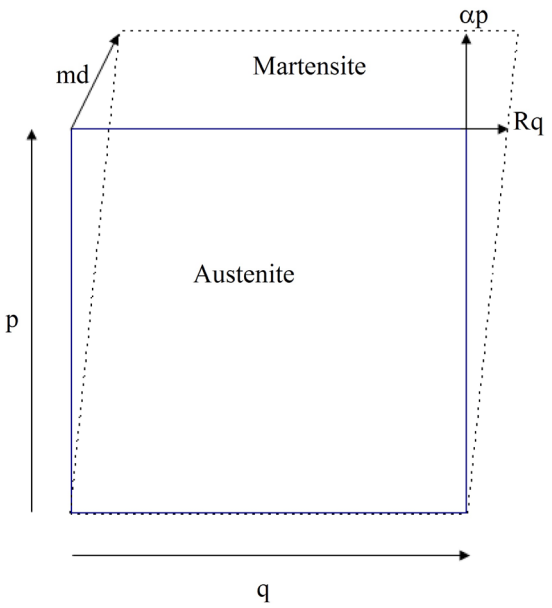

Fig. 1. Schematic representation of the most important parameters utilized in the crystallographic theory of martensitic phase transformation.

3. EXPERIMENTAL PROCEDURE

The materials used as starting material in this study were TRIP800 steel sheets with two different chemical compositions and initial thicknesses (Table 1). X-ray diffraction experiments were carried out using Phillips X'pert diffractometer with Cu-k_α radiation. The 2θ step size was equal to 0.02º and the exposure time was 53 seconds during X-ray peak scanning. The samples were mechanically and chemically polished, respectively for 30 minutes using a 95%H_2O_2-5%HF solution, [22], before radiation. The (111), (200) and (220) peaks of the austenite phase and the (110), (200) and (211) peaks of the ferrite phase were selected for further analysis.

The microstructure of the initial and as-deformed specimens were studied using scanning electron microscope (SEM). The polished specimens using the procedure recommended by Buehler Ltd., [22] were subsequently etched with 2% Nital solution. Leo 1430 scanning electron microscope with operating voltage of30 kV was used for microstructural examination. Tensile specimens with the gage length and width of 25 and 6.25 mm, respectively, were cut from the steel sheets by wire electro discharge machining to avoid the strain induced martensitic transformation during sample preparation. Tensile tests were then conducted using a screw-driven Zwick Z250 universal tensile testing machine with a constant cross head speed of 10 mm/min corresponding to an initial strain rate of 6.67×10^{-3} s^{-1}.

Table1. Chemical composition (in wt.%) and initial thickness of the investigated steels.

Steel	Fe	C	Si	Mn	P	Al	Initial thickness (mm)
TRIP1	Balance	0.22	1.55	1.65	0.012	0.04	1.5
TRIP2	Balance	0.32	1.4	1.5	0.008	0.047	1

[DOI: 10.22068/ijmse.17.1.109]

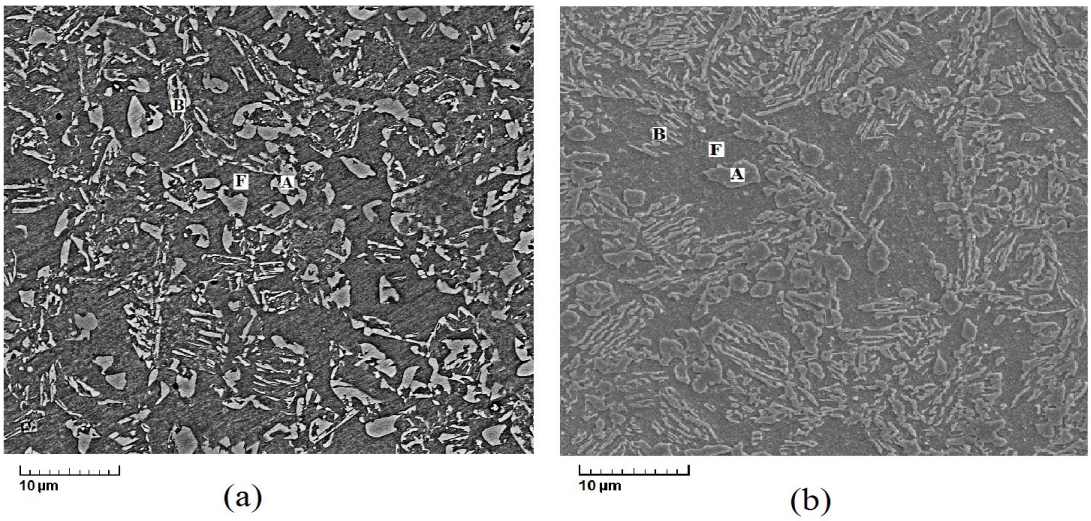

Fig. 2. SEM micrographs of the studied TRIP800 steels:
(a) TRIP1 (b) TRIP2; Bainite (B), retained austenite (A) and ferrite (F).

The finite element model using the real microstructure of the TRIP800 low alloy steels, [8-10, 13], was employed in this investigation. The SEM micrographs of the studied materials shown in Fig. 2 (a and b) were used for the subsequent image processing and importing to the ABAQUS general purpose commercial finite element code. The volume fraction and morphology of the constituent phases in Fig. 2 which have been considered as the representative volume elements, are very similar to those of the investigated materials.

Two dimensional three-node plane stress elements (CPS3) were adopted for discretization of the representative volume elements. The flat shape of the prepared tensile specimens and in-plane loading of these specimens during uniaxial, biaxial and plane strain tensile tests; make plane stress elements appropriate for discretization. In the discretized micrographs illustrated in Fig.3, the phase boundaries were modeled with finer meshes.

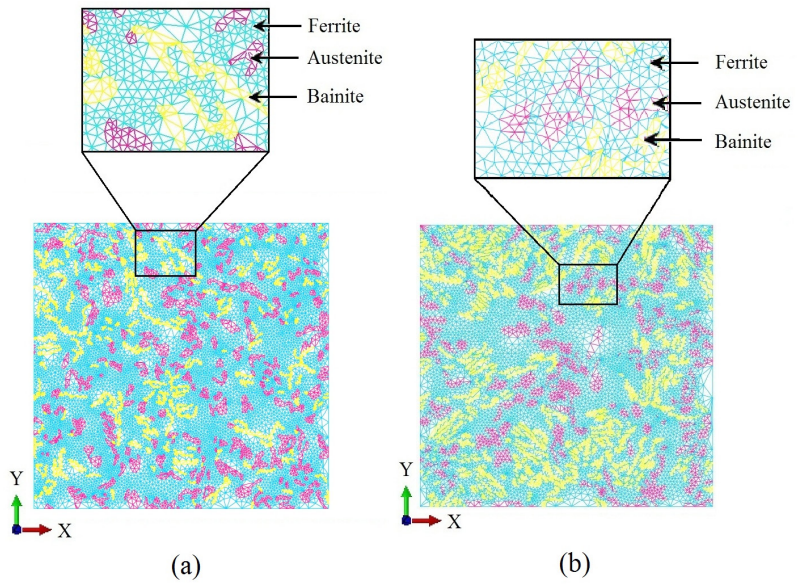

Fig. 3. The representative volume elements (RVE) which have been developed
for the TRIP800 steels investigated in this study (the blue, pink and yellow areas represent the ferrite, retained austenite and bainite phases, respectively): (a) TRIP1 (b) TRIP2.

[DOI: 10.22068/ijmse.17.1.109]

In the simulation of uniaxial tensile loading, the same displacement was applied on the nodes located along the right edge of each of the representative volume elements in the *x* direction, while these nodes could move freely in the *y* direction. The nodes located in the left edge of the representative volume elements were considered to be fixed in *x* direction, but were allowed to move freely in the *y* direction. The top and bottom edges of the elements were constrained so that all the nodes located along the edges displace the same in the y direction to preserve the rectangular shape of the representative volume elements during deformation. To model the biaxial tensile deformation, the nodes located along the left and bottom edges of the representative volume elements were considered not to move in the *x* and *y* directions, while the right and top edges of the element were subjected to displacements along the respective *x* and *y* directions based on the corresponding principal strain ratio, $\varepsilon_{22}/\varepsilon_{11}$. In the case of equi-biaxial deformation, for example, the right and top edges of the elements were displaced in the respective *x* and *y* directions so that the element experiences the same strain along the *x* and *y* directions. Macroscopic engineering stresses were obtained by dividing the reaction forces of the right and top edges of the volume element in the respective *x* and *y* directions by the corresponding initial dimensions. Macroscopic engineering strains were also calculated by dividing the right and top edge displacements by the initial length of the respective horizontal and vertical edges of the representative volume element.

All of the constituent phases of the TRIP steels were assumed to have isotropic elastic-plastic deformation behavior. The Young's modulus and Poisson's ratio of the constituent phases were considered to be 210 GPa and 0.3, respectively [8-10]. The flow stresses of ferrite and bainite phases were assumed to be estimated by the Ludwik-Hollomon equation (Equation 13). The flow curves of retained austenite and martensite in the

Table 2. Values of the materials parameters [8, 9, 23].

TRIP1		**TRIP2**	
Ferrite		**Ferrite**	
E (GPa)	210	E (GPa)	210
ν	0.3	ν	0.3
K	1200	*K*	1200
σ_v (MPa)	425	σ_v (MPa)	425
n	0.6	n	0.6
Bainite		**Bainite**	
E(GPa)	210	*E*(GPa)	210
ν	0.3	ν	0.3
K	3400	*K*	3400
σ_y (MPa)	500	σ_y (MPa)	500
n	0.65	*n*	0.65
Austenite		**Austenite**	
E(GPa)	210	*E*(GPa)	210
ν	0.3	ν	0.3
K	1910	σ_{y0}	700
σ_y (MPa)	570	H_0	50
n	0.64	n	0.24
Martensite		**Martensite**	
E(GPa)	210	*E*(GPa)	210
ν	0.3	ν	0.3
K	2000	σ_{y0}	2300
σ_y (MPa)	3200	H_0	100
n	1	*n*	0.05

[DOI: 10.22068/ijmse.17.1.109]

steel containing 0.3 wt.% C were predicted by the Swift equation (Equation 14) while those of steel with 0.22 wt.% C were estimated by the Ludwik-Hollomon equation. The material constants of these equations were assumed to be equal to those reported in the literature obtained by the in situ techniques in TRIP 800 steels with similar chemical compositions and microstructures [8, 9, 23]. Since the ferrite and bainite phases were not distinguished from each other in reference 23, the reported value for the flow stress of the ferrite in this reference cannot be used in this study. Instead, the values employed for prediction of flow stress as a function of plastic strain in references 8 and 9 have been adopted for the purpose of simulations in this work. The chemical compositions of ferrite phase in all low alloy TRIP steels are almost similar [24], and this is the case for bainite phase as well, therefore, the flow behavior of these phases has been assumed to be almost the same in both of the studied TRIP steels.

$$\sigma = \sigma_y + k\varepsilon^n \quad (13)$$

$$\sigma = \sigma_y (1 + H\varepsilon)^n \quad (14)$$

All the parameters in Equations 13 and 14 for the investigated steels, obtained from the literature, are given in Table 2.

Although the chemical compositions and microstructures of the studied TRIP 800 steels and those of the TRIP steels reported in the literature are similar, there are small fluctuations in the alloy compositions between the studied materials and those reported in the relevant references. Moreover, the grain size for each of the constituent phase is not necessarily the same in the studied and reported materials. Engineering stress- strain curves of the studied TRIP steels together with those reported in the references 8 and 25 for steels with chemical compositions and microstructure similar to those of the respective TRIP 1 and TRIP 2 steels are shown in Figs 4a and b. As it is clear from these figures, there is a good correlation between stress-strain curves of the studied materials and those reported in the literature. Therefore, the material constants reported in the literature for each of the constituent phases in the TRIP steels

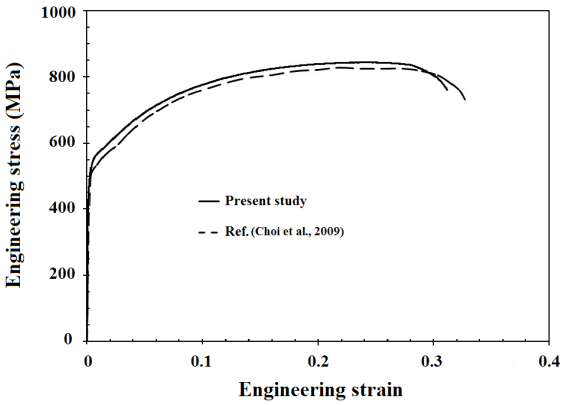

(a)

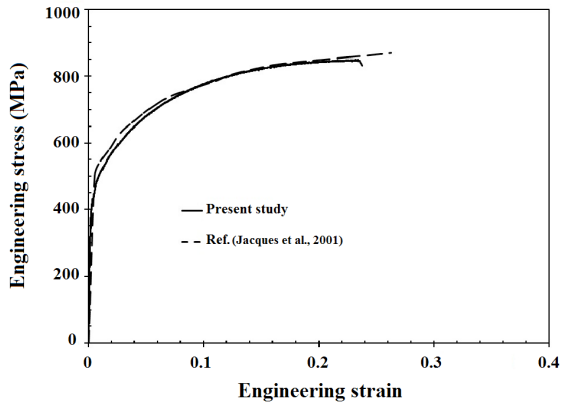

(b)

Fig. 4. Uniaxial engineering stress-strain curves of the studied materials together with those which reported for steels with similar microstructure and chemical composition: (a) TRIP1 (b) TRIP2.

with chemical compositions and microstructures similar to those of the studied materials can be used for simulation of the mechanical behavior of the investigated steels with a great confidence.

The kinetics of strain induced martensitic transformation expressed by Equation 1 was implemented into ABAQUS general purpose finite element code using a user material subroutine (UMAT). In this subroutine, the current magnitude of the mechanical driving force for martensitic transformation in each integration point of the elements belonging to the austenite phase is compared with the critical value of the mechanical driving force for the transformation and the mechanical properties of the integration point changes into those of the martensite phase, whenever the current mechanical driving force exceeds the critical one.

[DOI: 10.22068/ijmse.17.1.109]

4. RESULTS AND DISCUSSIONS

The X-ray diffraction patterns of the investigated steels in both the as-received and uniaxially deformed (fractured) conditions are shown in Fig. 5. This figure clearly indicates that the as-received samples contain both the BCC ferrite (α) and the FCC austenite (γ) phases. After uniaxial deformation, all of the diffraction peaks for the γ phase except for the peak corresponding to the (111) plane disappear which is an evidence for the occurrence of strain induced martensitic transformation.

The average lattice parameters of the austenite and ferrite phases can be determined by the experimental mean diffraction angles, $2\theta_i$, corresponding to each $\{hkl\}$ plane using the following relation [26]:

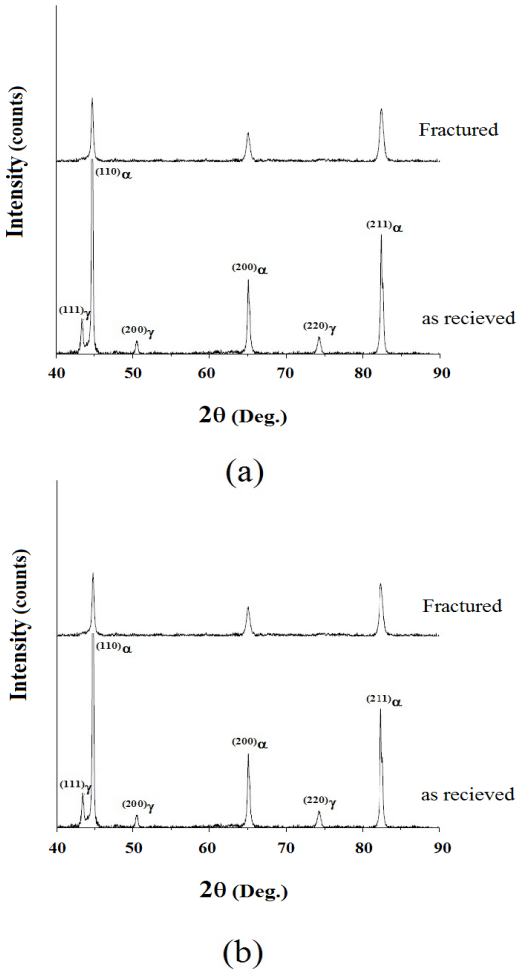

Fig. 5. X-ray diffraction patterns of microstructures of the as-received and uniaxially deformed state (fractured) TRIP800 steels: (a) TRIP1 (b) TRIP2.

$$a = \frac{1}{N}\sum_{i=1}^{N}\left(\frac{\lambda}{2}\right)\frac{\sqrt{h^2+k^2+l^2}}{\sin\theta_i} \tag{15}$$

In this equation, N is the number of diffractions and λ is the wavelength of incident X-ray beam. The average carbon content (in weight percent) of the austenite phase, C_γ, can be estimated using the following equation [27]:

$$a_\gamma = 0.35467 + 0.00467C_\gamma \quad \text{(nm)} \tag{16}$$

where, a_γ is the austenite lattice parameter.

The martensite lattice parameters are related to the average carbon content of the parent austenite phase through the following empirical equations [26]:

$$\begin{aligned} a_{\alpha'} &= a_\alpha - 0.0014C_\gamma \quad \text{(nm)} \\ c_{\alpha'} &= a_\alpha + 0.0115C_\gamma \quad \text{(nm)} \end{aligned} \tag{17}$$

where, $a_{\alpha'}$ and $c_{\alpha'}$ are the lattice parameters of the martensite phase and a_α is the lattice parameter of the ferrite phase.

The volume fraction of retained austenite can be obtained from the relative intensities of multiple diffraction peaks using the following equation [28]:

$$V_\gamma = \frac{\frac{1}{q}\sum_{j=1}^{q}\left(\frac{I_{\gamma j}}{R'_{\gamma j}}\right)}{\frac{1}{q}\sum_{j=1}^{q}\left(\frac{I_{\gamma j}}{R'_{\gamma j}}\right)+\frac{1}{p}\sum_{i=1}^{p}\left(\frac{I_{\alpha i}}{R'_{\alpha i}}\right)} \tag{18}$$

where, V_γ is the austenite volume fraction, $I_{\alpha i}$ and $I_{\gamma j}$ are the integrated intensities corresponding to the i^{th} and j^{th} peaks of the respective ferrite and austenite phases.

The value of R' parameter corresponding to each of the constituent phases can be expressed as follows [28, 29]:

$$R' = \left(\frac{1}{v^2}\right)\left[|F|^2 p\left(\frac{1+\cos^2 2\theta}{\sin^2\theta\cos\theta}\right)e^{-2M}\right] \tag{19}$$

where, v is the volume of unit cell, F the structural factor, p the multiplicity factor, θ the Bragg angle

[DOI: 10.22068/ijmse.17.1.109]

Table 3. The lattice parameters of different phases (α: ferrite, γ: austenite and α': martensite) and the volume fractions and carbon contents of retained austenite in the investigated steels.

Volume fraction of retained austenite (%)			a_g(nm)	a_a (nm)	C_g (wt.%)	$a_{a'}$ (nm)	$c_{a'}$ (nm)
	X-ray diffraction	Image analysis					
TRIP1	16	15	0.36003	0.28663	1.141	0.285013	0.2997
TRIP2	18	19	0.36014	0.286315	1.18	0.28467	0.2998

and e^{-2M} denotes the temperature factor.

The average lattice parameters of the constituent phases together with the average carbon content and volume fraction of the retained austenite in as-received condition estimated by both the XRD results and those of image analysis for both of the investigated steels are listed in Table 3.

Using the estimated lattice parameters of the austenite and martensite phases, the Bain strain, habit plane, shape deformation matrix, coordinate transformation matrix, and the parameters R and α of martensitic phase transformation were calculated based on the aforementioned corresponding formulae for both of the studied materials. These values are as follows:

$$(\gamma B\gamma)_{\text{TRIP1}} = \begin{pmatrix} 1.119544 & 0 & 0 \\ 0 & 1.119544 & 0 \\ 0 & 0 & 0.832431 \end{pmatrix} \quad (20)$$

$$(\gamma B\gamma)_{\text{TRIP2}} = \begin{pmatrix} 1.11786 & 0 & 0 \\ 0 & 1.11786 & 0 \\ 0 & 0 & 0.832454 \end{pmatrix} \quad (21)$$

Habit plane:

$$(-0.18332 \quad -0.81158 \quad -0.55474)_{\text{TRIP1}} \quad (22)$$

$$(-0.17724 \quad -0.80657 \quad -0.56394)_{\text{TRIP2}} \quad (23)$$

$$(\gamma P\gamma)_{\text{TRIP1}} = \begin{pmatrix} 0.9929 & -0.0312 & -0.0213 \\ 0.026 & 1.1153 & 0.0788 \\ -0.0214 & -0.0946 & 0.9354 \end{pmatrix} \quad (24)$$

$$(\gamma P\gamma)_{\text{TRIP2}} = \begin{pmatrix} 0.9935 & -0.0298 & -0.0208 \\ 0.0249 & 1.1133 & 0.0792 \\ -0.0209 & -0.0953 & 0.9334 \end{pmatrix} \quad (25)$$

$$(\gamma J\alpha')_{\text{TRIP1}} = \begin{pmatrix} 0.5713 & 0.5402 & 0.0973 \\ -0.5477 & 0.5674 & 0.0725 \\ -0.0193 & -0.1138 & 0.8237 \end{pmatrix} \quad (26)$$

$$(\gamma J\alpha')_{\text{TRIP2}} = \begin{pmatrix} 0.5700 & 0.5401 & 0.0957 \\ -0.5474 & 0.5660 & 0.0730 \\ -0.0177 & -0.1129 & 0.8237 \end{pmatrix} \quad (27)$$

$$R_{\text{TRIP1}} = 0.18 \quad (28)$$

$$R_{\text{TRIP2}} = 0.18 \quad (29)$$

$$\alpha_{\text{TRIP1}} = 0.043 \quad (30)$$

$$\alpha_{\text{TRIP2}} = 0.04 \quad (31)$$

As the calculated numerical values show, from the crystallographic point of view the TRIP phenomenon in the two studied steels is almost identical. The calculated values of R and α parameters agree well with those reported in the literature for similar steels [17].

In the present investigation, the critical driving force of the martensitic transformation has been considered to be the same as the thermodynamic free energy change for this transformation per unit volume. Based on the estimated carbon content of retained austenite (Table 3), the molar fraction of carbon in this phase are obtained to be approximately 0.051 and 0.052 for TRIP1 and TRIP2 steels, respectively. The thermodynamic free energy change of martensitic phase transformation for the aforementioned values of carbon in the austenite is then estimated to be 1340 J/mole for both of the steels [13, 30]. Dividing this value by the molar volume of austenite results in the critical driving force of martensitic transformation, i.e. 190 MPa. The molar volume of austenite can be obtained by its estimated lattice parameter.

The variation of retained austenite volume fraction as a function of the applied strain, determined experimentally, shows that the maximum transformation rate occurs in TRIP1

[DOI: 10.22068/ijmse.17.1.109]

steel during equi-biaxial tension, whereas for the case of TRIP2 plane strain tension has the greatest transformation rate. The transformation rate in uniaxial tension is less than that of plane strain tension for TRIP1, and equi-biaxial for TRIP2 [17, 31]. The values of stress state sensitivity parameter of martensitic phase transformation, k, were determined for the investigated steels so that the variations of retained austenite volume fraction as a function of applied strain predicted by the introduced stress invariant martensitic phase transformation kinetics model correlate with those reported in the literature for steels with similar chemical compositions and microstructure. These values were found to be 0.06 and 0.15 for the case of TRIP1 and TRIP2 steels, respectively.

Retained austenite volume fraction change as a function of applied strain reported in the reference 17 has been obtained by XRD, whereas the continuous magnetic method was reported in reference 31. Since the measurement methods of retained austenite volume fractions in the references 17 and 31 are not the same and the chemical compositions of the steels studied in the current work are slightly different, the applicability of the data in the aforementioned references to estimate the k values of the investigated materials needs to be examined.

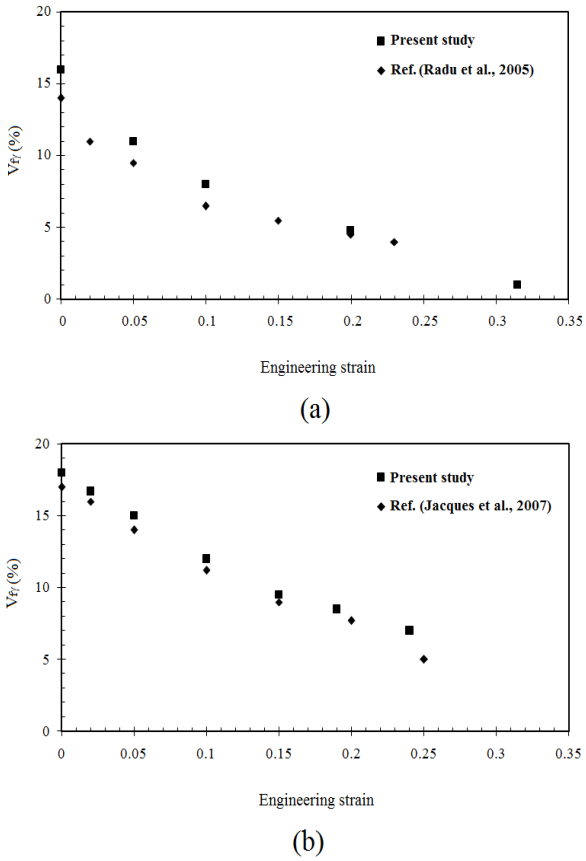

Fig. 6. Retained austenite volume fraction change as a function of applied strain in uniaxial tension of the studied materials and those which reported for steels with similar microstructure and chemical compositions: (a) TRIP1 (b) TRIP2.

Figs. 6 a and b show the retained austenite volume fraction change as a function of applied strain which occurs during uniaxial tension in TRIP 1 and TRIP2 steels measured by XRD together with those which reported in the references 31 and 17 for the same stress state, i.e., uniaxial tension. As these figures show, there is a good agreement between the measured retained austenite volume fractions and those reported in the relevant references. Therefore, it can be assumed that the transformation kinetics of the studied materials is very similar to those steels reported in the references 17 and 31, regardless of measuring method of retained austenite utilized in the references and the data in these references can be used for estimation of k value for the studied materials.

Fig. 7 shows the engineering stress-strain curve for both of the investigated materials obtained by the uniaxial tensile test together with the engineering flow curves predicted by the microstructure based finite element method. As these curves show, the yield and ultimate tensile strength of the two studied materials are almost the same, however, TRIP1 steel is more ductile than TRIP2. Since both the studied steels have almost the same austenite volume fraction and austenite carbon content, the difference in their flow behavior could be attributed to the different volume fractions of bainite in their microstructures. Comparing the experimental and calculated stress-strain curves, one can clearly see that there is a relatively good agreement between the experimental and the calculated results.

The volume fraction of retained austenite in both TRIP1 and TRIP2 steels as a function of the equivalent strain in the representative volume elements under different loading conditions estimated by the utilized model is given in Fig. 8. In addition, the experimental results from the corresponding literature of the volume fraction

[DOI: 10.22068/ijmse.17.1.109]

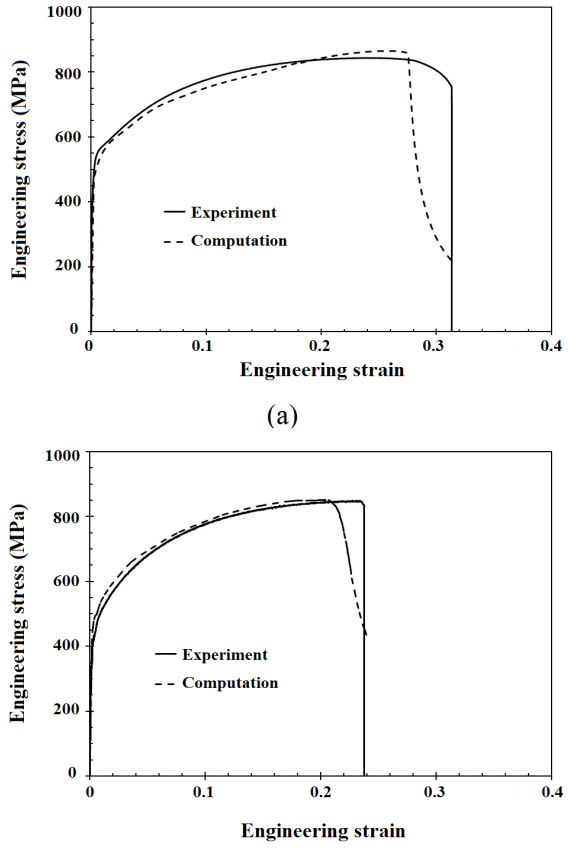

Fig. 7. Comparison of the calculated and experimental engineering stress- engineering strain curves in uniaxial tensile testing of TRIP800 steels: (a) TRIP1 (b) TRIP2.

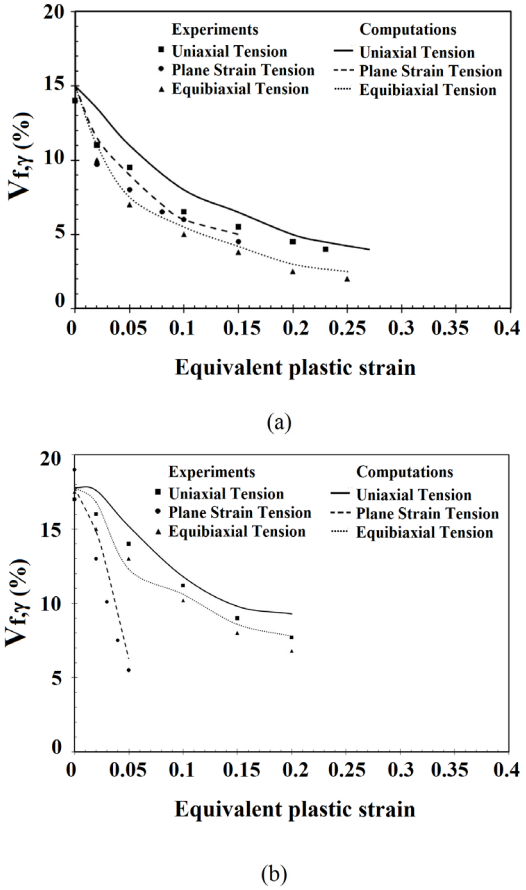

Fig. 8. Variations of the volume fraction of retained austenite as a function of applied strain in the representative volume elements together with a comparison with corresponding experimental results of TRIP800 steels: (a) TRIP1 (b) TRIP2.

of retained austenite as a function of equivalent strain obtained under the same loading conditions as those of the present study is superimposed on the curves in Fig. 6. As it is observable in this figure, the numerical results correlate well with the experimental results.

The variation of martensite volume fraction in the representative volume element has been estimated by image analysis. For example, the evolution of martensite phase in the representative volume element with the applied strain for both of the investigated steels during uniaxial tension is shown in Fig. 9. The red and blue areas in this figure represent the martensite and retained austenite phases, respectively. The remaining part of the microstructure is shown as white regions. The volume fraction of martensite and/or retained austenite can be estimated by the analysis of these digitized images using the same procedure as that used for determining the volume fraction of phases in a particular micrograph.

Fig. 8 shows that the stress state affects the strain induced martensitic phase transformation in the studied materials differently. Although the maximum transformation rate occurs during equi-biaxial tension in TRIP1 steel, this maximum value corresponds to plane strain tension for the case of TRIP2 steel. Since the carbon content of the retained austenite is almost identical in both of the studied steels, the martensite stability in these materials is very similar. Similar values for the critical driving force of martensitic phase transformation calculated for the investigated steels confirms that the stability of martensite phase in these steels is the same. Because the chemical composition of ferrite phase in all low

[DOI: 10.22068/ijmse.17.1.109]

alloy TRIP steels are almost the same [11, 24] and this is also the case for bainite phase, and due the fact that almost the same volume fraction of austenite is present in both steels, different amount of bainite phase in the microstructures of the investigated steels is the most probable cause for their different stress state sensitivity of martensitic phase transformation.

It has already been shown that the relative transformation rate of martensitic phase transformation in plane strain and equi-biaxial tension is related to the k parameter in Equation 1 [11]. Therefore, it can be said, according to the results of the present investigation, that the value of k might be dependent on the bainite volume fraction in the microstructure. The measurement

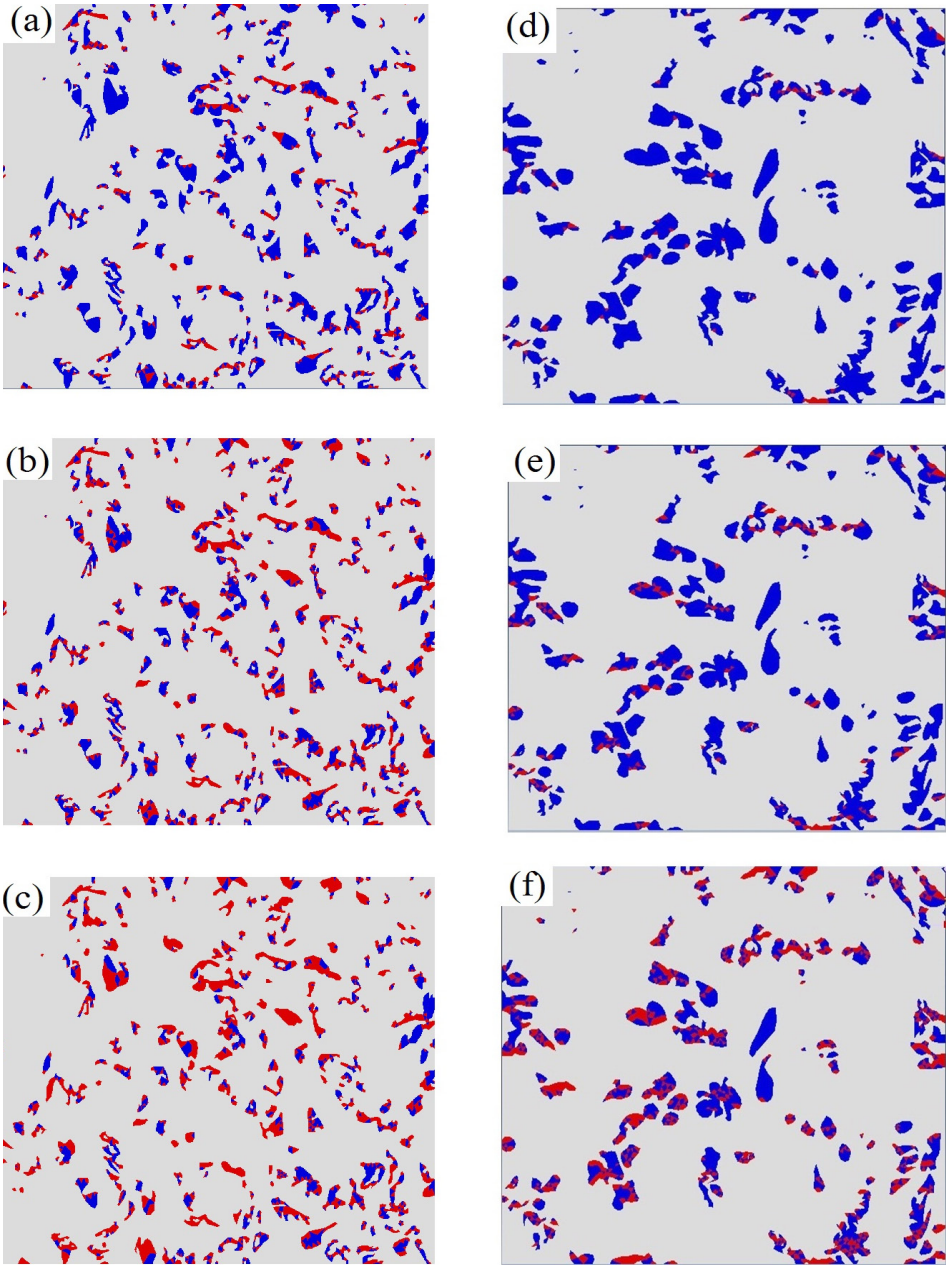

Fig. 9. The increase of martensite volume fraction in the RVEs with an increase in the engineering strain during uniaxial tensile loading of TRIP800 steels: The engineering strains are as follows: (a) 5%, (b) 15% and (c) 25% for TRIP1 Steel and (d) 2%, (e) 5% and (f) 15% for TRIP 2 steel. The martensite and retained austenite are shown as red and blue areas in the micrographs, respectively.

[DOI: 10.22068/ijmse.17.1.109]

of bainite volume fraction in the investigated steels showed that approximately 11-13 and 28-30 volume percent bainite phase is present in the microstructures of TRIP1 and TRIP2 steels, respectively. By comparing the volume fractions of these phases with corresponding values of the k parameter in Equation 1 obtained in this study, it can be said that the k parameter is almost equal to half of the bainite volume fraction.

The microstructure based finite element modeling of TRIP steels together with the stress invariant martensitic transformation kinetics law have been previously used as a virtual design tool [18]. The effects of various materials parameters on the mechanical behavior of TRIP steels have been investigated in the above mentioned study. For this purpose, each of the parameters was changed while the others kept constant and the effect of the changing parameter on the TRIP steel mechanical behavior was investigated. The results of the current work and pervious study conducted by the authors [13], show that the stress invariant martensitic transformation kinetics equation constants are related to chemical composition, crystallographic parameters of austenite and martensite phases, and the microstructure of the studied material and cannot be changed independently. For example, if the stability of the austenite phase changes, based on the equations 16 and 17, the lattice parameters of both austenite and martensite phases will change; because the stability of austenite depends on its carbon content. Change of austenite and martensite lattice parameters leads to the changes in the values of both R and α parameters according to equations 2 to 12 and following the procedure described in the reference 13. If the average chemical composition of the TRIP steel stays constant, the volume fraction of bainite should be changed for changing the carbon content of austenite and its stability resulting from this change. Therefore by changing the stability of austenite phase, the value of k parameter is also changed. The application of the microstructure based finite element modeling of multiphase TRIP steels as a virtual design tool should be thus reconsidered according to the results of the current study.

6. CONCLUSION

An already developed microstructure-based finite element model was utilized for predicting uniaxial engineering stress-strain curve as well as the variation of martensite volume fraction in two different TRIP800 steels as a function of equivalent strain under various loading conditions. Dillational (α) and shear (R) strains generated in the studied materials due to phase transformation were estimated using the crystallographic theory of martensitic phase transformation. The critical driving force for martensitic phase transformation which was assumed to be the same as the thermodynamic free energy change of the transformation per unit volume was calculated for both of the investigated steels. The stress state sensitivity parameter for the martensitic phase transformation, k, was determined so that the variation of martensite volume fraction with the strain under various loading conditions was predicted satisfactorily. It was found that the critical driving force for martensitic phase transformation of the studied steels is almost the same, i.e. 190 MPa, however, their stress state sensitivities are different. The estimated value of k was determined to be 0.06 for the steel having 11 to 13 volume percent bainite and 0.15 for the steel with 28 to 30 volume percent bainite, respectively. Based on the results obtained from the present work, the value of k can be estimated to be almost equal to half of the bainite volume fraction in the investigated steel microstructure. Therefore, the bainite volume fraction can be used at least as a first guess for determining the stress state sensitivity parameter. Combining the results of the present study with those reported previously, all of the necessary parameters in the strain induced martensitic phase transformation model can be estimated at a priori and the microstructure based finite element model which has been developed already for predicting the mechanical behavior of TRIP800 steels can be utilized as a virtual design tool for developing multiphase TRIP steels having specified mechanical properties.

[DOI: 10.22068/ijmse.17.1.109]

ACKNOWLEDGEMENT

The authors would like to thank Ferdowsi University of Mashhad for financial support of this work.

Compliance with Ethical Standards: The authors declare that they have no conflict of interest.

REFERENCES

1. Muransky, O., Hornak, P., Lukas, P., Zrnik, J., and Sittner, P., "Investigation of retained austenite stability in Mn-Si TRIP steel in tensile deformation condition" J. Achiev. Mater. Manuf. Eng., 2006, 14, 26-30.
2. Marketz, F. and Fischer, F. D., "A micromechanical study on the coupling effect between microplastic deformation and martensitic transformation. Comput. Mater. Sci, 1994, 3, 307-325.
3. Reisner, G., Werner, E. A., Fischer, F. D., "Micromechanical modeling of martensitic transformation in random microstructures" Int. J. Solids Struct., 1998, 35, 2457-2473.
4. Leblond, J. B., "Mathematical modelling of transformation plasticity in steels II: Coupling with strain hardening phenomena" Int. J. Plast., 1989, 5, 573-591.
5. Leblond, J. B., Devaux, J. and Devaux, J. C., "Mathematical modelling of transformation plasticity in steels I: Case of ideal-plastic phases" Int. J. Plast., 1989, 5, 551-572.
6. Taleb, L. and Sidoroff, F., "A micromechanical modeling of the Greenwood–Johnson mechanism in transformation induced plasticity" Int. J. Plast., 2003, 19, 1821-1842.
7. Han, H. N., Lee, C. G., Oh, C.S., Lee, T. H. and Kim, S. J., "A model for deformation behavior and mechanically induced martensitic transformation of metastable austenitic steel" Acta Mater., 2004, 52, 5203-5214.
8. Choi, K. S., Liu, W. N., Sun, X., Khaleel, M. A., "Microstructure-based constitutive modeling of TRIP steel: Prediction of ductility and failure modes under different loading conditions" Acta Mater., 2009, 57, 2592-2604.
9. Choi, K. S., Liu, W. N., Sun, X., Khaleel, M. A., Ren, Y. and Wang, Y. D., "Advanced micromechanical model for transformation-induced plasticity steels with application of in-situ high-energy X-ray diffraction method" Metall. Mater. Trans. A, 2008, 39, 3089-3096.
10. Soulami, A., Choi, K. S., Liu, W. N., Sun, X., Khaleel, M. A., Ren, Y., Wang, Y. D.,"Predicting fracture toughness of TRIP 800 using phase properties characterized by in-situ high-energy x-ray diffraction" Metall. Mater. Trans. A, 2010, 41, 1261-1268.
11. Cherkaoui, M., Soulami, A., Zeghloul, A., Khaleel, M.A.,"A phenomenological dislocation theory for martensitic transformation in ductile materials: From micro-to macroscopic description" Philos. Mag., 2008, 88, 3479-3512.
12. Serri, J., Cherkaoui, M., "Constitutive modeling and finite element analysis of the formability of TRIP steels" J. Eng. Mater.T., 2008, 130, 031009-1-031009-13.
13. Hosseinabadi, F., Rezaee-Bazzaz, A., Mazinani, M., "Finite Element Simulation of Mechanical Behavior of TRIP800 Steel Under Different Loading Conditions Using an Advanced Microstructure-Based Model", Metall. Mater. Trans. A, 2017, 48, 930-942.
14. Furnemont, Q., "The micromechanics of TRIP-assisted multiphase steels ", PhD thesis, Université Catholique de Louvain, Belgium, 2003.
15. Hecker, S. S., Stout, M. G., Staudhammer, K. P., Smith, J. L., "Effects of strain state and strain rate on deformation-induced transformation in 304 stainless steel: Part I. Magnetic measurements and mechanical behavior", Metall. Mater. Trans. A, 1982, 13, 619-626.
16. Murr, L., "Strain-induced dislocation emission from grain boundaries in stainless steel", Mater. Sci. Eng., 1981, 51, 71-79.
17. Jacques, P. J., Furnémont, Q., Lani, F., Pardoen, T., Delannay, F., "Multiscale mechanics of TRIP-assisted multiphase steels: I. Characterization and mechanical testing", Acta Mater., 2007, 55, 3681-3693.
18. Choi, K. S., Soulami, A., Liu, W. N., Sun, X., Khaleel, M. A., "Influence of various material design parameters on deformation behaviors of TRIP steels", Comput. Mater. Sci, 2010, 50, 720-730.
19. Bhadeshia, H., "Geometry of crystals", Institute of Materials, London, 2001, 51-69.
20. Kundu, S., "Transformation strain and crystallographic texture in steels", PhD thesis, University of Cambridge, United Kingdom, 2007.
21. Christian, J. W., "The theory of transformations in metals and alloys", Newnes, 2002.
22. Mazinani, M. and Poole, W., "Effect of martensite plasticity on the deformation behavior of a low-carbon dual-phase steel", Metall. Mater. Trans. A, 2007, 38, 328-339.

[DOI: 10.22068/ijmse.17.1.109]

23. Delannay, L., Jacques, P., Pardoen, T., "Modelling of the plastic flow of trip-aided multiphase steel based on an incremental mean-field approach", Int J Solids Struct., 2008, 45, 1825-1843.
24. Bhadeshia, H. and Edmonds, D., "The bainite transformation in a silicon steel", Metall. Mater. Trans. A, 1979, 10, 895-907.
25. Jacques,P., Furnemont, Q., Pardoen, T., Delannay, F., "On the role of martensitic transformation on damage and cracking resistance in TRIP-assisted multiphase steels", Acta Mater., 2001, 49, 139-152.
26. Van Dijk, N. H., Butt, A. M., Zhao, L., Sietsma, J., Offerman, S. E., Wright, J. P., Van der Zwaag, S., "Thermal stability of retained austenite in TRIP steels studied by synchrotron X-ray diffraction during cooling", Acta Mater., 2005, 53, 5439-5447.
27. Zhang, M. Y., Zhu, F. X. and Zheng, D. S., "Mechanical properties and retained austenite transformation mechanism of TRIP-aided polygonal ferrite matrix seamless steel tube", J. Iron Steel Res. Int., 2011, 18, 73-78.
28. E975-03, S. A., E975-03 "Standard practice for x-ray determination of retained austenite in steel with near random crystallographic orientation", ASTM, West Conshohocken, PA, 2008.
29. Cullity, B. D., "Elements of X-ray Diffraction", Addison-Wesley, Massachusetts, United States, 1978.
30. Bhadeshia, H., "Driving force for martensitic transformation in steels", Met. Sci. J., 1981, 15, 175-177.
31. Radu, M., Valy, J., Gourgues, A. F., Le Strat, F., Pineau, A., "Continuous magnetic method for quantitative monitoring of martensitic transformation in steels containing metastable austenite", Scr. Mater., 2005, 52, 525-530.

[DOI: 10.22068/ijmse.17.1.109]